Desalination 404 (2017) 112–120

Contents lists available at ScienceDirect

Desalination

journal homepage: www.elsevier.com/locate/desal

A low-temperature multi-effect desalination system powered by the cooling water of a diesel engine

Fengming Zhang [a,*], Shiming Xu [b], Dongdong Feng [b], Shunquan Chen [a], Ruxu Du [c], Chuangjian Su [a], Boya Shen [a]

[a] Guangzhou Institutes of Advanced Technology, Chinese Academy of Sciences, 511458 Guangzhou, China
[b] School of Energy and Power Engineering, Dalian University of Technology, 116024, Dalian, China
[c] Institute of Precision Engineering, The Chinese University of Hong Kong, Shatin, N. T., Hong Kong SAR, China

HIGHLIGHTS

- A 60 T/d LT-MED desalination system powered by diesel engine waste heat was designed.
- A compact and integrated four-effect tower distiller was proposed and built.
- The desalination plant was operated successfully and tested comprehensively.
- Electricity and water co-production can provide for islands and offshore platforms.

ARTICLE INFO

Article history:
Received 24 July 2016
Received in revised form 23 October 2016
Accepted 5 November 2016
Available online 14 November 2016

Keywords:
Electricity and freshwater co-generation
Low-temperature multi-effect distillation
Waste heat recovery
Diesel engine

ABSTRACT

This paper introduces a medium-size low-temperature multi-effect desalination (LT-MED) system. Powered by the cooling water of a 1000 kW diesel power generator set, the system can produce 60 tons of fresh water per day. First, the thermodynamic and heat transfer model of the LT-MED system is derived. Second, an integrated four-effect tower distiller is designed and built. The system is installed in the Guishan Island, Zhuhai, Guangdong, China, and tested comprehensively. In the operation, the evaporation temperature of each effect is linearly proportional to the heat load of the power generator. Additionally, the evaporation temperature in each effect distiller rose linearly when the heat load was gradually increased. The variation of evaporation pressure was consistent with the evaporation temperature. When the heat load of the power generator increases from 300 kW to 530 kW, the fresh water production rate increases from 1.26 m^3/h to 2.30 m^3/h. The conductivity of the fresh water is usually < 100 μS/cm. Because of electricity and freshwater co-production, the system is environmental friendly and is particularly useful for islands and offshore platforms.

1. Introduction

With the rapid growth of the global population and the improvement of living standards, the demand for freshwater has increased dramatically in the past few decades. As a result, global water scarcity has become a critical problem [1–2]. To solve this problem, desalination is a key technology. In the past 50–60 years, desalination industry has grown dramatically [3–4]. However, there is a crucial problem: high energy consumption. In general, desalination processes can be divided into two main categories based on the phase change of seawater [5–8]. The first category refers to thermal processes including Multi-Stage Flash distillation (MSF), Multi-Effect Distillation (MED), Thermal Vapor Compression (TVC), and Mechanical Vapor Compression (MVC). The second category is based membrane filtration including reverse osmosis (RO), and electro-dialysis (ED). From the energy point of view, all these desalination processes are energy thirsty [9–11]. In particularly, the membrane process would have a higher overall efficiency at the expense of consuming a large amount of electricity. The greatest advantage of the thermal processes is that they can use any types of thermal sources consuming very little electricity. As a result, it is particularly useful when renewable energy, such as solar, geothermal, as well as waste heat, such as streams and/or hot water from power generation and other chemical engineering processes, is available. In short, it has been agreed that the desalination process shall use renewable energy or waste energy that is low cost or even cost free [12–15].

Waste thermal energy is very common in the process industry, and waste heat management is an important consideration as it affects operation cost and system performance. In general, waste heat can be

* Corresponding author.
E-mail address: fm.zhang@giat.ac.cn (F. Zhang).

http://dx.doi.org/10.1016/j.desal.2016.11.006
0011-9164/

Nomenclature

Abbreviations

A	heat transfer area m^2
BPE	the rise in brine's boiling point rise, °C
CFU	colony-forming units
Cp	specific heat capacity $kJ \cdot kg^{-1} \cdot K^{-1}$
d	diameter, m
F	flow rate, $kg \cdot h^{-1}$
g	gravitational acceleration, $m \cdot s^{-2}$
h	specific enthalpy, $kJ \cdot kg^{-1}$
H	head of delivery, m
L	effective length of the tubes, m
LT-MED	low-temperature multi-effect distillation
MED	multi-effect distillation
MSF	multi-stage flash distillation
MVC	mechanical vapor compression
N	number of effect, number of columns
NTU	nephelometric turbidity unit
Nu	Nusselt number
P	pressure, kPa
Pr	Prandtl constant
Q	heat load, kW
R	fouling resistance of pipe wall, $m^2 \cdot K^{-1} \cdot W^{-1}$
Re	Reynolds number
RO	reverse osmosis
T	temperature, K
TVC	thermal vapor compression
X	seawater concentration, ppm

Greek letters

α	heat transfer coefficiency, $w \cdot m^{-2} \cdot K^{-1}$
κ	total heat transfer coefficient, $w \cdot m^{-2} \cdot K^{-1}$
ρ	density, $kg \cdot m^{-3}$
γ	latent heat, $kJ \cdot kg^{-1}$
λ	heat conductivity coefficient,$w \cdot m^{-2} \cdot K^{-1}$
ν	kinematic viscosity, $m^2 \cdot s^{-1}$
Γ	spray density, $kg \cdot m^{-1} \cdot s^{-1}$
μ	dynamic viscosity, $Pa \cdot s$
Δ	difference
Δt	heat transfer temperature difference, K
ΔT_{pre}	temperature difference in the hot side of the preheater, K
ε	concentration ratio

Subscripts

cw	cooling water
fw	fresh water
hw	hot water
i	the *i*th effect
in	inlet, inner
L	liquid
out	outlet, outer
s	saturated
sw	sea water
v	vapor
vap	vapor
w	tube wall

divided into two kinds: high grade and low grade. The high grade refers to those that have temperature above 80 °C and can be easily recovered using conventional methods, while low grade refers to those that have temperature below 80 °C and is often not economically viable to recover [16–17]. In practice, low grade waste heat would be one of the most promising options for desalination [18–19]. It matches well with the requirement of MED, in which higher temperature should be avoided to prevent the precipitation of gypsum that could severely foul the heat exchanger [20–21].

Diesel generator set consisting of engine, generator and control system, is widely used in the region far away from power grid such as islands and offshore platforms. However, it can only convert about 40% of the energy from fuel combustion into useful work, and the remaining energy is discharged into environment in the form of waste heat, which includes 30% in the exhaust gas, 25% in the jacket cooling water, and 5% of other heat losses [22]. Thus, utilizing the waste heat from diesel engine for desalination would be ideal [23–25]. This motivates us to design and build a 60 Ton per day (T/day) LT-MED desalination system powered by a 1000 kW diesel generator set.

The rest of the paper is organized as follows: Section 2 presents the design of the desalination system. Section 3 gives its thermodynamic model. Section 4 describes the building of the system and the experiment results. Finally, Section 5 contains conclusions and discussions.

2. Pilot plant description

2.1. Design conditions

The desalination process was designed based on the waste heat resource and the quality of raw seawater. The cooling water waste heat of a diesel engine with a rated power of 1000 kW was used as the heat sources of the MED desalination process, and the related parameters of the diesel engine were listed in Table 1. The temperature range of cooling water produced in the diesel engine is usually between 71 and 85 °C, which matches extremely well with the multi-effect distillation (MED) technology. Considering the heat dissipation and fluctuating electric load, the waste heat load of cooling water recovered from the diesel engine was set as 600 kW. Besides, the quality of raw seawater was also tested before designing the system, which is listed in Table 2 and a simple pretreatment process will be sufficient for MED technology.

2.2. Process description

The schematic diagram of our LT-MED seawater desalination process driven by cooling water waste heat from a diesel generator set is shown in Fig. 1. It consists of a hot water circuiting system, four evaporators, a condenser, a vacuum system and other auxiliary equipment. In the four-effect distiller, each effect contains heat exchanging tubes, vapor space, brine spray nozzles and a demister. The horizontal falling film evaporator is preferred to use in the MED processes for getting high heat transfer efficiency [26–27].

As shown in the figure, after being filtered by a simple meshed grid the seawater is pumped into the tubes of the condenser. A large portion of the seawater is rejected back to the sea as cooling water, while the remnant flows into the preheater through a self-cleaning filter. Then, the preheated water enters the first effect distiller starting the multi-effect desalination process. At the meantime, the circulating hot water

Table 1
Parameters of the diesel engine.

Parameters	Unit	Value
Engine type	–	S12R-PTA2
Rated load	kW	1000
Thermal load of the cooling water	kW	697
Cooling water flow	$L \cdot min^{-1}$	1650
Temperature adjustment range	°C	71–85
Maximum temperature	°C	98

Table 2
The raw seawater quality.

Number	Indexes	Unit	Test result
1	Turbidity	NTU	<1
2	Chroma	°	<5
3	suspended solids	mg/l	17.5
4	Smell	–	Not detected
5	Visible substances	–	Not detected
6	pH	–	7.94
7	Electrical conductivity	mS/cm	45.0
8	Total dissolved solids	mg/l	3.8×10^4
9	Chemical oxygen demand	mg/l	48.2
10	Aerobic bacterial count	CFU/ml	257
11	Total coliform group	CFU/ml	Not detected
12	Heat resistant *Escherichia coli* group	CFU/100 ml	Not detected
13	*Escherichia coli*	CFU/100 ml	Not detected

receives the heat from the cooling water of the diesel engine and pumps into the first effect distiller as heating medium to transfer the heat energy to the feed seawater, and flows into the preheater to preheat the feed.

This forward feed configuration is adopted for its simplicity and operation efficient [28]. The entire low-temperature evaporation process is operated under low pressure condition generated by a vacuum pump. Both the brine and the vapor flow from the first effect to the last effect. At the first effect distiller, the feed seawater is heated up to its boiling temperature and a portion of it evaporates subsequently. The generated vapor goes through demister and then flows into the second effect distiller to be condensed. In the second effect distiller, the condensation and the evaporation occurs at the same time. This permits the feed seawater to undergo multiple boiling without additional heating. This process is repeated likewise in the third and the fourth effect distillers. Finally, the generated vapor in the last effect distiller is condensed in the condenser. The condensed freshwater from each effect distiller is pumped into a storage tank and the brine is pumped back to the sea.

3. Mathematical model

3.1. Modeling assumption

In this section, the mathematical model of mass balance and energy balance for the preheater, the evaporators and the condenser are presented. In the model, following assumptions are made:

- The startup and shutdown conditions are not considered, so the process is assumed to be at steady state and the parameters do not depend on time.
- Concentration of feed seawater is known based on sample analysis, and the concentration of salt in distillate stream is negligible, so distillate product is assumed to be salt free.
- Since all effects follow almost the same structural design, temperature difference between each two adjacent effects is taken to be identical.
- The outer side walls of preheater, evaporators and condenser are insulated, heat losses to the surrounding are assumed to be negligible.
- Pressure drop in the demister as well as during the vapor condensation process is neglected.
- The effect of fouling factors and the presence of non-condensable gasses on the heat transfer coefficients in the evaporators, preheaters and the condenser are neglected.

3.2. Thermodynamic calculation model

A schematic of main four-effect desalination plant's parts is shown in Fig. 2.

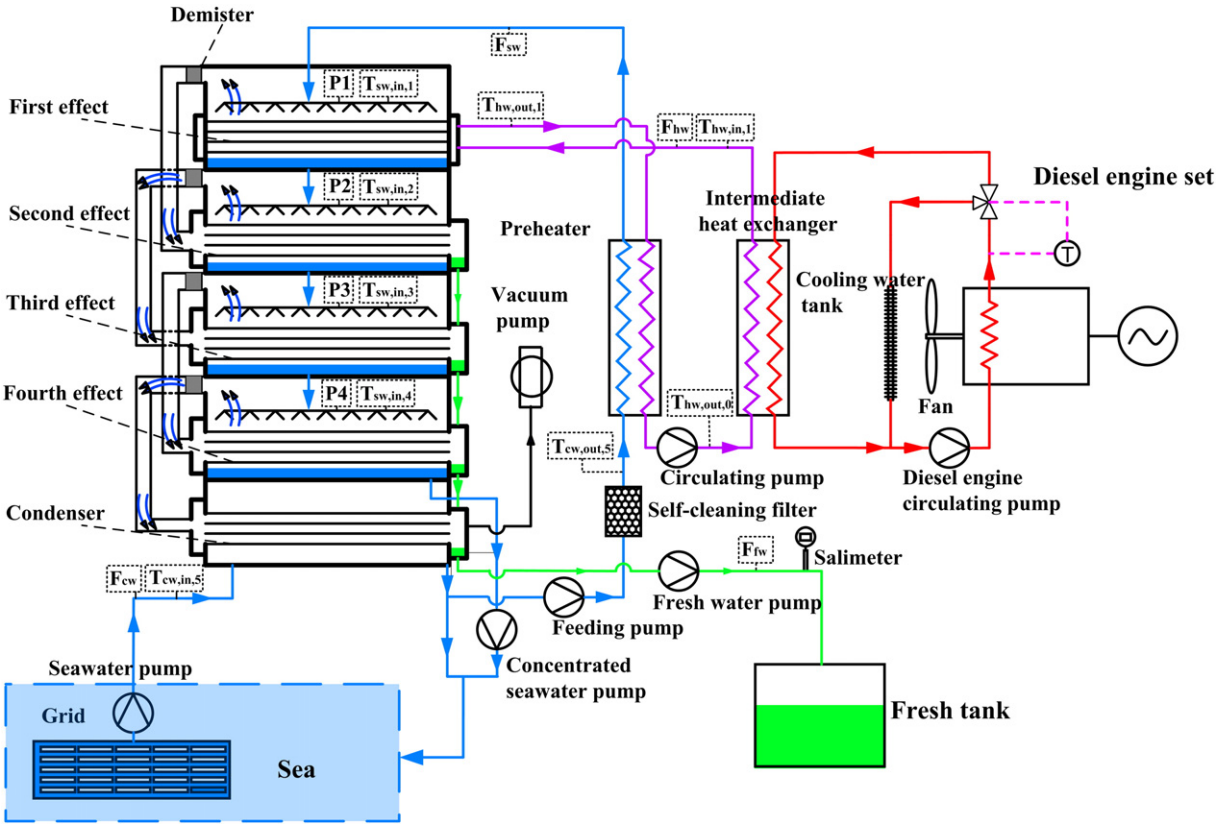

Fig. 1. Schematic diagram of the LT-MED system, the line colors show the temperature gradients from low (blue) to high (red).

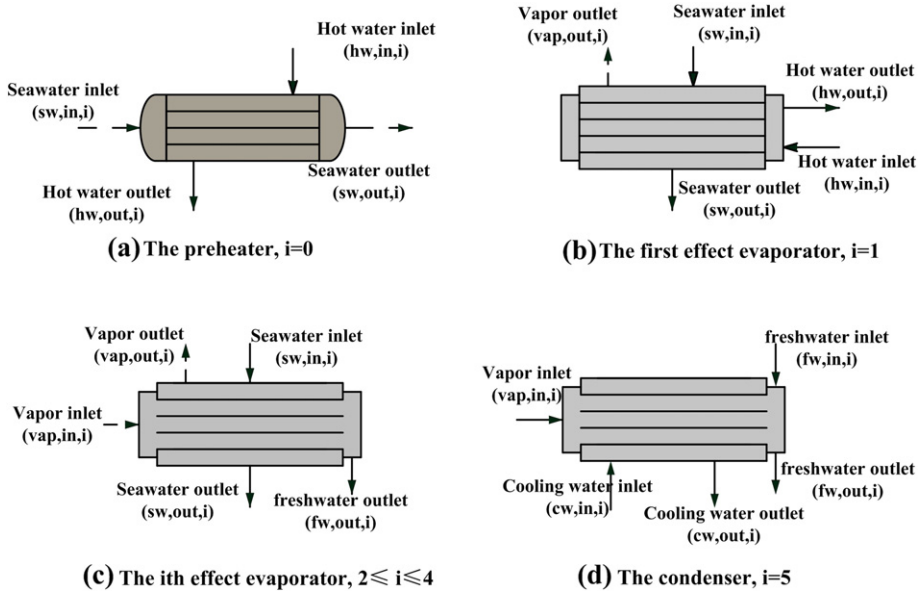

Fig. 2. Control volume MED parts.

As seen in Fig. 2a, the mass and energy balance equations for preheater ($i = 0$) are as follows:

$$F_{sw,in,i} = F_{sw,out,i} \tag{1}$$

$$F_{hw} = F_{hw,in,i} = F_{hw,out,i} \tag{2}$$

$$Q_i = F_{hw,in,i}(h_{hw,in,i} - h_{hw,out,i}) = F_{sw,in,i}(h_{sw,out,i} - h_{sw,in,i}) \tag{3}$$

As seen in Fig. 2b, the mass and energy balance equation for the first effect ($i = 1$) is written as:

$$F_{hw} = F_{hw,out,i} = F_{hw,in,i} = F_{hw,in,i-1} \tag{4}$$

$$F_{sw,in,i} = F_{sw,out,i} + F_{vap,out,i} \tag{5}$$

$$T_{hw,out,i} = T_{hw,in,i-1} \tag{6}$$

$$T_{sw,in,i} = T_{sw,out,i-1} \tag{7}$$

$$T_{vap,out,i} = T_{sw,in,i} - BPE \tag{8}$$

$$Q_i = F_{hw}(h_{hw,in,i} - h_{hw,out,i}) = F_{sw,out,i}h_{sw,out,i} + F_{vap,out,i}h_{vap,out,i} - F_{sw,in,i}h_{sw,in,i} \tag{9}$$

The BPE at a given pressure refers to the increase in boiling temperature due to the dissolution of salts in the water, and $h_{vap,out,i}$ has considered gasification latent heat and enthalpy difference due to temperature change. The BPE can be calculated by Eq. (10) according to literature [29]:

$$BPE = AX + BX^2 + CX^3 \tag{10}$$

$$A = 8.325 \times 10^{-2} + 1.883 \times 10^{-4}T + 4.02 \times 10^{-6}T^2 \tag{11}$$

$$B = -7.625 \times 10^{-4} + 9.02 \times 10^{-5}T - 5.2 \times 10^{-7}T^2 \tag{12}$$

$$C = 1.522 \times 10^{-4} - 3 \times 10^{-6}T - 3 \times 10^{-8}T^2 \tag{13}$$

where X is salinity and T is seawater temperature. Besides, the total heat load recovered from the cooling water of the diesel engine can be calculated as follow.

$$Q_{hw} = Q_0 + Q_1 \tag{14}$$

The mathematic models for ith effect ($2 \le i \le 4$, Fig. 2c) is expressed as

$$F_{vap,in,i} = F_{vap,out,i-1} = F_{fw,out,i} \tag{15}$$

$$F_{sw,in,i} = F_{sw,out,i} + F_{vap,out,i} \tag{16}$$

$$T_{vap,in,i} = T_{vap,out,i-1} \tag{17}$$

$$T_{sw,in,i} = T_{sw,out,i-1} \tag{18}$$

$$T_{vap,out,i} = T_{sw,in,i} - \Delta T - BPE \tag{19}$$

$$Q_i = F_{vap,in,i}(h_{vap,in,i} - h_{fw,out,i}) = F_{sw,out,i}h_{sw,out,i} + F_{vap,out,i}h_{vap,out,i} - F_{sw,in,i}h_{sw,in,i} \tag{20}$$

The mathematic models for condenser ($i = 5$, Fig. 2d) is expressed as

$$F_{vap,in,i} = F_{vap,out,i-1} = F_{fw,out,i} \tag{21}$$

$$F_{cw} = F_{cw,in,i} = F_{cw,out,i} \tag{22}$$

$$T_{vap,in,i} = T_{vap,out,i-1} = T_{fw,out,i} \tag{23}$$

$$Q_i = F_{vap,in,i}(h_{vap,in,i} - h_{fw,out,i}) = F_{cw,out,i}(h_{cw,out,i} - h_{cw,in,i}) \tag{24}$$

Total water production:

$$F_{fw} = \sum_{i=2}^{5} F_{fw,out,i} \tag{25}$$

A calculation program was developed based on Eqs. (1) to (25), and the flowchart of the thermodynamic calculation for the desalination is presented in Fig. 3.

Table 3 presents the known and calculated thermodynamic state parameters, and the maximum freshwater production for the system is 2848 kg/h, that is over 60 T/d.

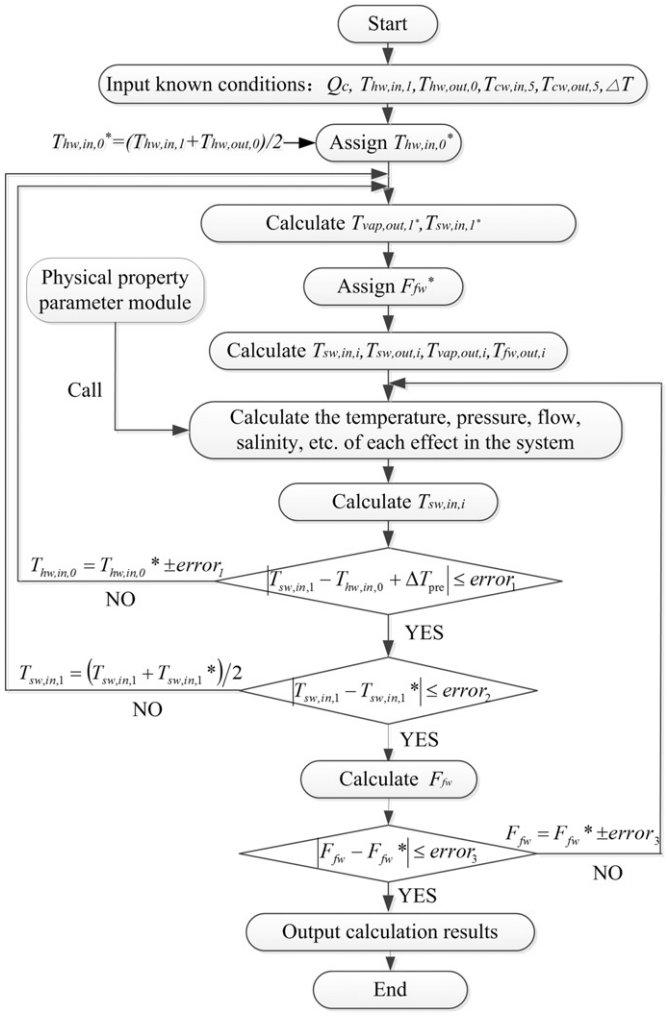

Fig. 3. The block diagram of thermodynamic calculation.

3.3. Heat transfer model

Based on the above thermodynamic state parameters, heat transfer coefficients of every effect distiller are described by the following equations [30–32], and the detailed structural parameters can be determined by heat transfer calculation. Specifically, internal convection and external falling film evaporation happen in first effect, internal condensation and external falling film evaporation occur from the second to the fourth effect, and internal convection and external condensation happen in the condenser.

Heat transfer coefficient of falling film evaporation on horizontal tube bundle can be expressed as follows,

$$\alpha_{i,out}=0.032\left({\lambda_L}^3 g/\nu_L^2\right)^{\frac{1}{3}}\left(4\Gamma_i/\mu_L\right)^{0.3367}\mathrm{Pr}^{0.4629} \tag{26}$$

$$\Gamma_i=F_i/(L_i\cdot N_i) \tag{27}$$

Heat transfer coefficient of condensation in horizontal tube is described by,

$$\alpha_{i,in}=0.555\left\{\lambda_L^3\rho_L(\rho_L-\rho_v)g\left[r+\frac{3}{8}c_{p,L}(T_s-T_w)\right].[\mu_L d_{in}(T_s-T_w)]\right\}^{\frac{1}{4}} \tag{28}$$

Heat transfer coefficient of single phase flow in horizontal tube is given by,

$$Nu_i=0.023\mathrm{Re}_L^{0.8}\mathrm{Pr}_L^{n} \tag{29}$$

where $n=0.4$, if the fluid is heated, otherwise, $n=0.3$.

Heat transfer coefficient of condensation on horizontal tube bundle is described by

$$\alpha_{out}=0.725\left[\frac{gr{\rho_L}^2\lambda_L^3}{\mu_L d_{out}N(T_s-T_w)}\right]^{\frac{1}{4}} \tag{30}$$

Thermal load of ith effect distiller is given by

$$Q_i=\kappa_i A_i\Delta t_i \tag{31}$$

Table 3
Thermodynamic state parameters for the desalination systems.

Symbol	Parameter	Unit	Value	Remarks[a]
Q_c	Heat load recovered from the cooling water of the diesel engine	kW	600	–
$Q_{c,0}$	Heat load of the preheater	kW	195.4	–
$Q_{c,1}$	Heat load of the first effect	kW	404.6	–
N	Numbers of effect	–	4	–
ε	Concentration ratio	–	2	–
ΔT	Temperature difference between two adjacent effects	°C	6	–
ΔT_{pre}	Temperature difference in the hot side of the preheater	°C	3	–
F_{cw}	Cooling water flow rate	kg/h	79,051.6	$F_{cw,in,5}$, $F_{cw,out,5}$
F_{sw}	Feed seawater flow rate	kg/h	7000	$F_{sw,in,0}$, $F_{sw,out,0}$, $F_{sw,in,1}$
F_{hw}	Hot water flow rate	kg/h	36,814.3	$F_{hw,in,0}$, $F_{hw,out,0}$, $F_{hw,in,1}$, $F_{hw,out,1}$
F_{fw}	Fresh water flow rate	kg/h	2848.54	–
$T_{cw,in,5}$	Cooling water condenser inlet temperature	°C	30	$T_{cw,in,5}$
$T_{cw,out,5}$	Cooling water condenser outlet temperature	°C	36	$T_{cw,out,5}$
$T_{sw,in,1}$	first effect evaporator spray temperature	°C	60	$T_{sw,out,0}$
$T_{sw,in,2}$	second effect evaporator spray temperature	°C	54	$T_{sw,in,2}$
$T_{sw,in,3}$	third effect evaporator spray temperature	°C	48	$T_{sw,in,3}$
$T_{sw,in,4}$	fourth effect evaporator spray temperature	°C	42	$T_{sw,in,4}$
$T_{hw,in,1}$	Hot water inlet temperature in the first effect evaporator	°C	74	$T_{hw,in,1}$
$T_{hw,out,1}$	Hot water outlet temperature in the first effect evaporator	°C	64.56	$T_{hw,in,0}$
$T_{hw,out,0}$	Hot water outlet temperature in the preheater	°C	60	–
P1	Pressure of the first effect evaporator	kPa	19.9479	–
P2	Pressure of the second effect evaporator	kPa	15.0321	–
P3	Pressure of the third effect evaporator	kPa	11.1903	–
P4	Pressure of the fourth effect evaporator	kPa	8.21989	–

[a] Parameters with same values in the mathematical model are shown in the remarks column.

Table 4
The structure parameters.

Heat exchanger	Tube bundles (row × column)	Evaporation temperature/°C	Mean temperature difference/°C	Calculated heat transfer area/m^2	Actual heat transfer area/m^2
First effect	13 × 16	60	8.36	21.99	23.28
Second effect	18 × 16	54	6	31.13	32.23
Third effect	21 × 16	48	6	36.23	37.60
Fourth effect	24 × 16	42	6	41.96	42.98
Condenser	15 × 16	/	8.66	26.13	26.86

The effective heat transfer coefficient of *i*th effect distiller is written by

$$\kappa_i = \left[\left(R_{in} + \frac{1}{\alpha_{i,in}}\right)\frac{d_{out}}{d_{in}} + \frac{d_{out}}{2\lambda}\ln\left(\frac{d_{out}}{d_{in}}\right) + \left(R_{out} + \frac{1}{\alpha_{i,out}}\right)\right]^{-1} \quad (32)$$

Based on the design conditions and parameters given above as well as the MED mathematical model of thermodynamics and heat transfer calculation, the actual heat exchange area and the tube bundle arrangement in each effect distiller are obtained by the layout design of structure. The detailed structure parameters of the desalination plant are listed in Table 4.

In order to provide compact and integrated desalination equipment for usage on islands and offshore platforms, an integrated four-effect tower distiller was designed (Fig. 4). Heat transfer tubes (i.d./o.d. 17/19 mm) were made of stainless steel 316L, with the effective length of 1.95 m, and the total number of heat exchanging tubes was up to 1500. The overall size of the four-effect distiller was 2.5 m × 2.0 m × 4.0 m (length × width × height) and the total weight was about 5.6 tons. The liquid distributors consisting of runoff tubes and liquid distributing salvers was designed to distribute liquid film uniformly on the heat exchanging tube bundles. Besides, multi-stage baffles were used as demisters.

4. Auxiliary equipment and measuring apparatus

According to the thermodynamic parameters of the desalination system, some auxiliary equipments were selected to build the pilot plant. On the basis of the local seawater quality, terrain, and ocean currents, coastal seawater intake system was chosen, and a submersible pump with a grille was selected to delivery raw seawater. The self-cleaning filter (filtration precision ≤ 100 μm) was adopted to further filter seawater. Water-ring vacuum pump was used to keep the pressure of the distillation process at a low level (with an extreme pressure of 3.3 kPa).

Resistance thermometers, pressure sensors, and orifice plate flow meters were used to measure temperature, pressure, and flow rate in the pilot plant respectively. Specially, sea water spray temperature and generated vapor pressure in each effect distiller must be measured in order to compare with the data in listed in Table 3. The quality of water product was monitored by an online conductivity meter installed at outlet of the product pump. Besides, off-line freshwater sample was collected and detected based on the national drinking water criterion [33]. Detailed information for auxiliary equipment and measuring apparatus can be found in Table 5. All of the data shown during the working process were recorded by the host computer automatically. Detailed location distribution and numbering order of the measurement points can be seen in Fig. 1.

5. Operating performance of demonstration system

5.1. Pilot plant

The high production (60T/d) desalination pilot plant driven by cooling water waste heat of the diesel engine has been established and successfully operated since early 2015. Fig. 5 shows the photo of pilot device. The diesel generator set combines with the desalination pilot plant provides an electricity and water co-production for residents of Guishan Island.

5.2. Startup procedure

It is important to startup the desalination plant quickly and economically. We usually start the pilot plant after the diesel generator set is

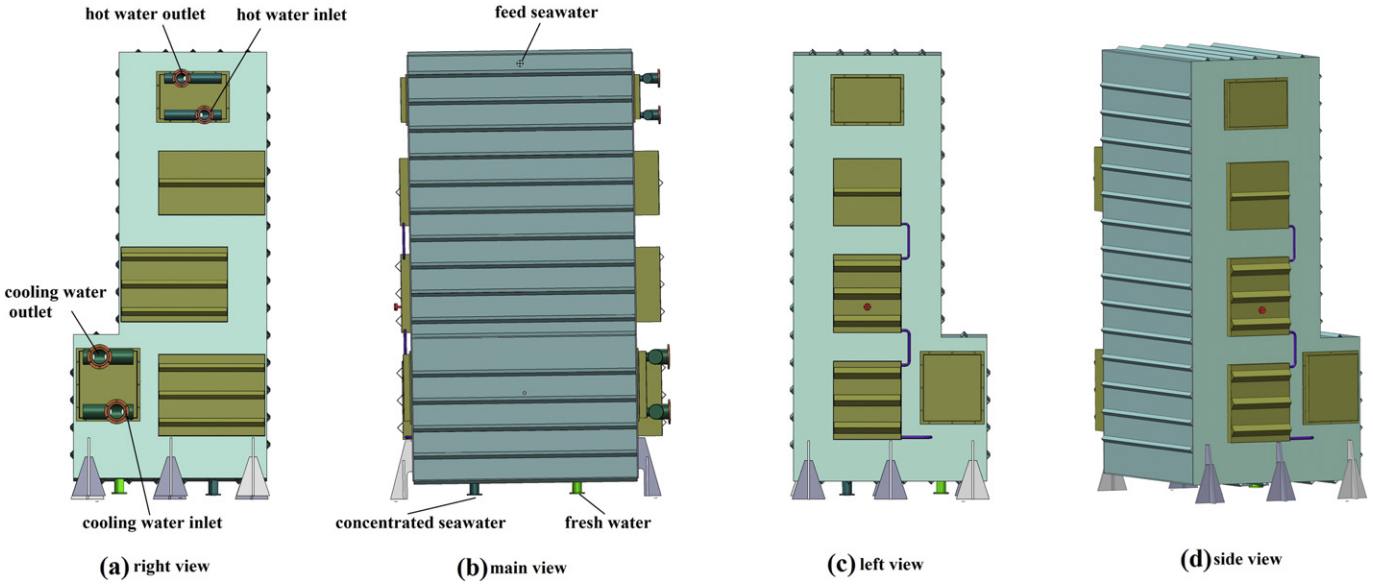

Fig. 4. Structural diagram of the four-effect distiller.

Table 5
Summary of auxiliary equipment and measuring apparatus.

Item	Models	Specifications	Supplier
Seawater pump	SP95-3-B	F = 100 m^3/h, H = 30 m	Grundfos
Feeding pump	CRN10-3	F = 10 m^3/h, H = 20 m	Grundfos
Fresh water pump	SS211-1.5H	F = 3.5 m^3/h, H = 12 m	NIKKISO
Concentrated seawater pump	SS211-1.5H	F = 4.5 m^3/h, H = 12 m	NIKKISO
Circulating pump	65–100(I)A	F = 38 m^3/h, H = 8 m	Shanghai Kaitong
Vacuum pump	2BVA2060	F = 0.45 m^3/min, extreme pressure: 3.3 kPa	Dongguan shengfei
Self-cleaning filter	ZL-LB1.5-1.6	10 m^3/h, filtration precision ≤ 100 μm	Wuxi public power
Salimeter	DDG-3080	0–1000 μS/cm, error < 0.1%	Shanghai Boqu
Resistance thermometer	PT100	−20–100 °C, error < 0.1%	Shanghai SPES
Pressure sensor	SP-851	0–100 kPa, error < 0.1%	Shanghai SPES
Orifice plate flow meter, F1	SKLG125	F = 0–120 m^3/h, error < 0.5%	Jinhu YIJIA
Orifice plate flow meter, F2	SKLG32	F = 0–10 m^3/h, error < 0.5%	Jinhu YIJIA
Orifice plate flow meter, F3	SKLG50	F = 0–50 m^3/h, error < 0.5%	Jinhu YIJIA
Orifice plate flow meter, F2	SKLG25	F = 0–5 m^3/h, error < 0.5%	Jinhu YIJIA

running, at which point the waste heat of cooling water starts to generate. When the diesel generator set runs and the cooling water temperature rises to about 65 °C, the hot water circulation pump is started to recover the waste heat. At the same time, the distiller is depressurized to 5–10 kPa by the water ring vacuum pump, and 20–30 min are usually needed to at this stage. And then, cooling water and the feed of seawater will be pumped to the condenser and the distiller respectively. Fig. 6 shows the parameters at the startup stage of the pilot plant.

The running diesel engine provides heat sources for the desalination system. The total heat load recovered by the pilot plant can be calculated by Eqs. (3), (9), and (14). It can be seen from Fig. 6a that $T_{h,in,1}$, $T_{h,out,1}$ and $T_{h,out,0}$ decline quickly first when the feed of seawater are injected into the distiller, which shows that heat has been transferred from the circulating hot water to the seawater. Then $T_{h,in,1}$, $T_{h,out,1}$ and $T_{h,out,0}$ rise and become stable gradually. As the feed evaporates and the steam condenses, the differences of temperature and pressure among the four effect distillers are established step by step (Fig.6b and c), which shows that the pilot plant has been operated successfully.

5.3. Temperature and pressure distribution at steady-state condition

The influence of heat load on evaporation temperature and pressure in each effect distiller is shown in Fig.7a and b, with constant flow rates of cooling seawater, feed seawater and circulating hot water. It can be seen that the evaporation temperature of each effect almost increases linearly when the heat load was gradually increased. This is due to the increase in circulating hot water temperature with the increase in heat load, which leads to the increase in evaporation temperatures in the first effect. And the evaporation temperature decreases gradually from the first effect to the last effect for throttle effect in the distiller. Since evaporation temperature in each effect is saturated, the variation of evaporation pressure is consistent with evaporation temperature.

5.4. Fresh water productivity and quality

Fig. 8 shows the effect of the heat load on freshwater production rate and conductivity. It can be seen that the water production rate will increase with increasing heat load. The designed heat load and water productivity of the desalination system are 600 kW and 2.84 m^3/h respectively. The heat load of the desalination system usually ranges from 300 kW to 530 kW, which corresponds to the operating power of the generator. Due to the limited power consumption of the residents, the quantity of heat is usually lower than full load. Thus, the heat transfer area of the distiller is sufficient in the insufficient heat load conditions and water productivity depends on the total heat load [34–35]. Under the operating conditions, water production rate is 1.26 m^3/h at heat load of 310 kW. When the heat load of desalination system increases to 530 kW, water production rate increases to 2.30 m^3/h. And the fresh water production may further increase when the heat load increases.

The distillation process can remove most of the salt in seawater, thus reducing the conductivity. The conductivity of seawater feed is usually kept as a constant, so desalination efficiency can be acquired by measuring conductivity of the fresh water. The power of the diesel generator is unstable because of the fluctuation in electricity consumption, which makes heat load unstable. Thus, the fresh water conductivity fluctuates

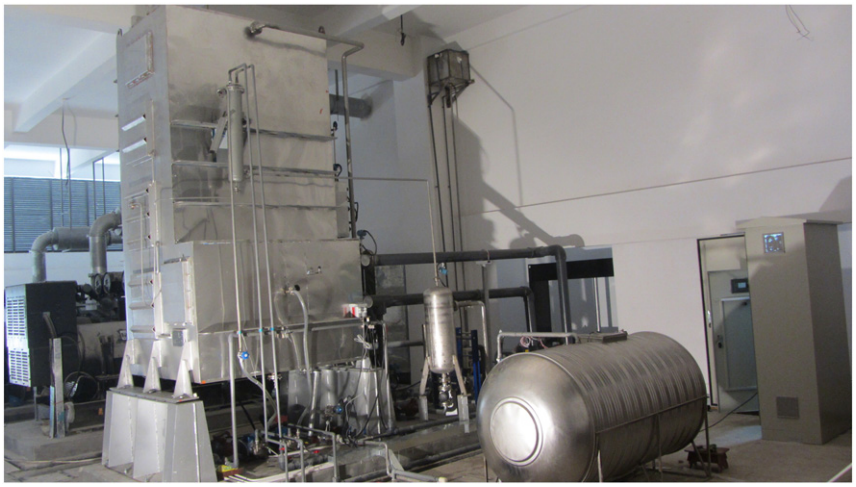

Fig. 5. Desalination pilot plant in Guishan Island.

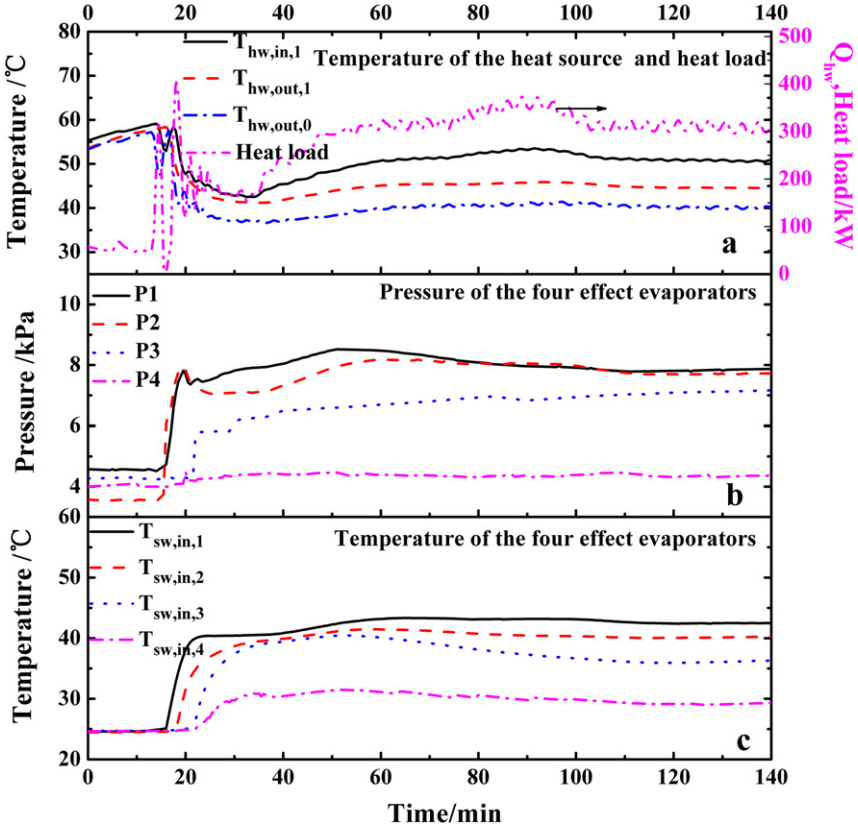

Fig. 6. The startup procedure of the pilot plant (F_{cw} = 45,000 kg/h, F_{sw} = 7000 kg/h, F_{hw} = 33,000 kg/h).

frequently. Considering the baffle demisters used in LT-MED system, an optimal vapor mass flow rate corresponding to the best working efficiency may exist [36–37]. It can be seen in Fig. 8 that the conductivity of fresh water fluctuates strongly due to fluctuation of vapor mass flow rate. Even so, the conductivity of desalted water is <100 μS/cm in most operating conditions.

Moreover, based on the third party testing result, the quality of the freshwater samples can be seen in Table 6. It meets the standard of the Chinese national drinking water act [33].

6. Conclusion

This paper presents a 60 Ton per day (T/d) low-temperature multi-effect distillation (LT-MED) desalination system driven by the cooling water waste of a 1000 kW diesel engine power generator. The system combines the diesel generator set forms an electricity-water coproduction plant, which can provide both electricity and freshwater for the residents of Guishan Island, Zhuhai, China. Based on the discussions above, following conclusions can be drawn:

(1) The performance of the system can be well predicted by the presented thermodynamic model.
(2) In the steady state operating condition, the evaporation temperature of each effect is proportional to the amount of heat load. The evaporation temperature decreases gradually from the first effect to the last effect. Besides, the variation of evaporation pressure is correlated to the evaporation temperature.
(3) The water production increases from 1.26 m^3/h to 2.30 m^3/h when the heat load is increased from 300 kW to 530 kW. The conductivity of the freshwater fluctuates due to the fluctuation of vapor mass flow rate, but is <100 μS/cm in most operating conditions. Moreover, based on the test of a third party company, the freshwater meet the standard of the Chinese national drinking water act and is very safe to drink.

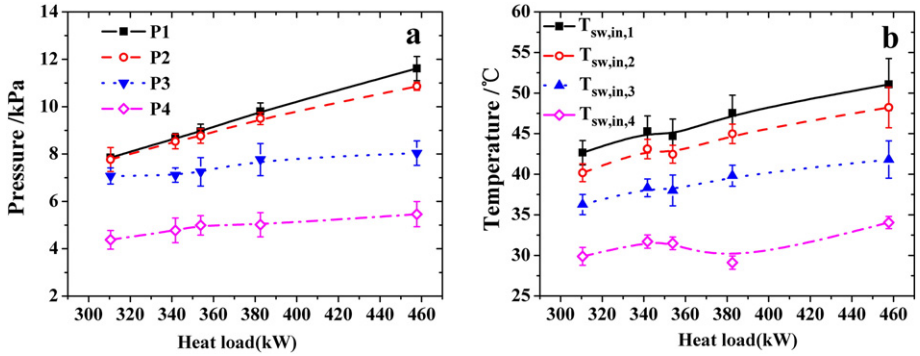

Fig. 7. Temperature and pressure distribution in the distiller at different heat loads.

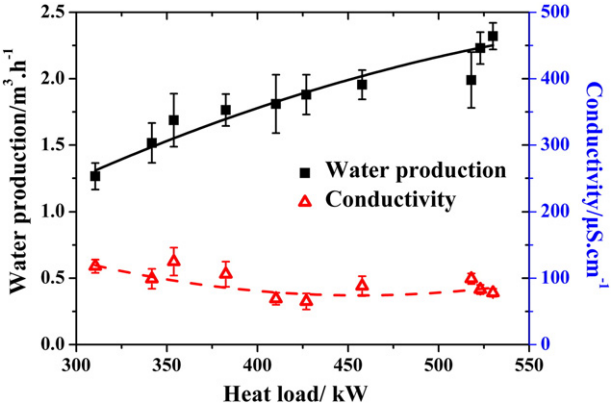

Fig. 8. Influence of heat load on freshwater production rate and conductivity.

Table 6
The detailed testing results of the freshwater.

Number	Testing item	Units	Testing results	Standards for drinking water
1	Turbidity	NTU	<1	≤1
2	Chroma	°	<5	≤15
3	Suspended solids	mg/l	1.5	–
4	Smell	–	No	No
5	Visible substances	–	No	No
6	pH	–	6.7	6.5–8.5
7	Electrical conductivity	μS/cm	121.2	–
8	Total dissolved solids	mg/l	76.3	≤1000
9	Chemical oxygen demand	mg/l	0.4	<5
10	Aerobic bacterial count	CFU/ml	21	≤100
11	Heat resistant *Escherichia coli* group	CFU/100 ml	Not detected	Not detected
12	Total coli group	CFU/100 ml	Not detected	Not detected
13	*Escherichia coli*	CFU/100 ml	Not detected	Not detected

Acknowledgement

This work is supported by Guangdong-Hongkong Breakthrough Bidding Project in Key Areas (NO. 2012A090200001), Research Project of High Tech Industry in Nansha District (NO. 2013P013), PhD Start-Up Fund of Natural Science Foundation of Guangdong Province (NO. 2014A030310203), Guangdong Province Science and Technology Plan Project (NO. 2013B091100003; NO. 2016B090918037), Nansha District Technology Development Project (NO. 2015KF013), Shenzhen Basic Research Project (NO. JCYJ20150316144639927), Shenzhen Technology Development Project (NO. 20150528141008015).

References

[1] A.D. Khawaji, I.K. Kutubkhanah, J.M. Wie, Advances in seawater desalination technologies, Desalination 142 (2008) 47–69.
[2] N. Ghaffour, T.M. Missimer, G.L. Amy, Technical review and evaluation of the economics of water desalination: current and future challenges for better water supply sustainability, Desalination 309 (2013) 197–207.
[3] M. Elimelech, W.A. Phillip, The future of seawater desalination: energy, technology, and the environment, Science 333 (2011) 712–717.
[4] A. Cipollina, G. Micale, L. Rizzuti, Seawater Desalination: Conventional and Renewable Energy Processes, Springer, 2009.
[5] S. Burn, M. Hoang, D. Zarzo, F. Olewniak, E. Campos, B. Bolto, O. Barron, Desalination techniques—a review of the opportunities for desalination in agriculture, Desalination 364 (2015) 2–16.
[6] N. Ghaffour, S. Lattemann, T. Missimer, K.C. Ng, S. Sinha, G. Amy, Renewable energy driven innovative energy-efficient desalination technologies, Appl. Energy 136 (2014) 1155–1165.
[7] L. Malaeb, G.M. Ayoub, Reverse osmosis technology for water treatment: state of the art review, Desalination 267 (2011) 1–8.
[8] A.D. Khawaji, I.K. Kutubkhanah, J.M. Wie, Advances in seawater desalination technologies, Desalination 221 (2008) 47–69.
[9] J.M. Gordon, C.H. Tong, Thermodynamic perspective for the specific energy consumption of seawater desalination, Desalination 386 (2016) 13–18.
[10] V.G. Gude, N. Nirmalakhandan, S. Deng, Renewable and sustainable approaches for desalination, Renew. Sustain. Energy Rev. 14 (2013) 2641–2654.
[11] A.G.M. Ibrahim, I. Dincer, A solar desalination system: exergetic performance assessment, Energy Convers. Manag. 101 (2015) 379–392.
[12] A. Al-Karaghouli, L.L. Kazmersk, Energy consumption and water production cost of conventional and renewable-energy-powered desalination processes, Renew. Sust. Energ. Rev. 24 (2013) 343–356.
[13] K.V. Reddy, N. Ghaffour, Overview of the cost of desalinated water and costing methodologies, Desalination 205 (2007) 340–353.
[14] M. Al-Nory, M. El-Beltagy, An energy management approach for renewable energy integration with power generation and water desalination, Renew. Energy 72 (2014) 377–385.
[15] N.A.S. Elminshawy, F.R. Siddiqui, G.I. Sultan, Development of a desalination system driven by solar energy and low grade waste heat, Energy Convers. Manag. 103 (2015) 28–35.
[16] K. Kwon, B.H. Park, D.H. Kim, D. Kim, Parametric study of reverse electrodialysis using ammonium bicarbonate solution for low-grade waste heat recovery, Energy Convers. Manag. 103 (2015) 104–110.
[17] R. Law, A. Harvey, D. Reay, A knowledge-based system for low-grade waste heat recovery in the process industries, Appl. Therm. Eng. 94 (2016) 590–599.
[18] Y. Ammar, H. Li, C. Walsh, P. Thornley, V. Sharifi, A.P. Roskilly, Desalination using low grade heat in the process industry: challenges and perspectives, Appl. Therm. Eng. 48 (2012) 446–457.
[19] X. Wang, A. Christ, K. Regenauer-Lieb, K. Hooman, H.T. Chua, Low grade heat driven multi-effect distillation technology, Int. J. Heat Mass Transf. 54 (25–26) (2011) 5497–5503.
[20] P. Fiorini, E. Sciubba, Modular simulation and thermoeconomic analysis of a multi-effect distillation desalination plant, Energy 32 (2007) 459–466.
[21] M.E. Kazemian, A. Behzadmehr, S.M.H. Sarvari, M.E. Kazemian, A. Behzadmehr, Thermodynamic optimization of multi-effect desalination plant using the DoE method, Desalination 257 (2010) 195–205.
[22] G. Shu, M. Zhao, H. Tian, H. Wei, X. Liang, Y. Huo, W. Zhu, Experimental investigation on thermal OS/ORC (Oil Storage/Organic Rankine Cycle) system for waste heat recovery from diesel engine, Energy 107 (2016) 693–706.
[23] K.S. Maheswari, K. Kalidasa Murugavel, G. Esakkimuthu, Thermal desalination using diesel engine exhaust waste heat–An experimental analysis, Desalination 358 (2015) 94–100.
[24] Y.F. Wang, S.M. Xu, Analysis of desalination system powered by waste heat from diesel generating set, Energy Conserv. Technol. 32 (2014) 455–460.
[25] N.A.S. Elminshawy, F.R. Siddiqui, G.I. Sultan, Development of a desalination system driven by solar energy and low grade waste heat, Energy Convers. Manag. 103 (2015) 28–35.
[26] L. Gong, S. Shen, H. Liu, M. Xingsen, C. Xue, Three-dimensional heat transfer coefficient distributions in a large horizontal-tube falling film evaporator, Desalination 357 (2015) 104–116.
[27] C.-Y. Zhao, W.-T. Ji, P.-H. Jin, W.-Q. Tao, Heat transfer correlation of the falling film evaporation on a single horizontal smooth tube, Appl. Therm. Eng. 103 (2016) 177–186.
[28] S. Ibrahim, I.W. Al-Mutaz, Comparative performance evaluation of conventional multi-effect evaporation desalination processes, Appl. Therm. Eng. 73 (2014) 1194–1203.
[29] H.T. El-Dessouky, H.M. Ettouney, Fundamentals of Salt Water Desalination, Elsevier Science, 2002 587.
[30] J.-S. Chiou, S.-a. Yang, C.'o.-K. Chen, Laminar film condensation inside a horizontal elliptical tube, Appl. Math. Model. 18 (1994) 340–346.
[31] X.L. Ren, Experimental Investigation on Heat Transfer Coefficients of Horizontal Tube Falling Film Evaporation, Dalian Dalian University of Technology, 2008 49–53.
[32] M.Z. Shi, Z.Z. Wang, Principle and Design of the Heat Exchanger, Southeast University Press, Nanjing, 2003 65–68.
[33] Standards for Drinking Water Quality, GB 5749, 2006.
[34] L. Yang, W. Wang, The heat transfer performance of horizontal tube bundles in large falling film evaporators, Int. J. Refrig. 34 (2011) 303–316.
[35] L. Xu, M. Ge, S. Wang, Y. Wang, Heat-transfer film coefficients of falling film horizontal tube evaporators, Desalination 166 (2004) 223–230.
[36] C. Galletti, E. Brunazzi, L. Tognotti, A numerical model for gas flow and droplet motion in wave-plate mist eliminators with drainage channels, Chem. Eng. Sci. 63 (2008) 5639–5652.
[37] L.I. Jia, H. Sufi, X. Wang Chin, Numerical study of steam-water separators with wave-type vanes, J. Chem. Eng. 15 (2007) 492–498.